The effect of crystal anisotropy on the Lamb Mossbauer recoilless fraction and second-order Doppler shift in zinc

1989 J. Phys.: Condens. Matter 1 5165

(http://iopscience.iop.org/0953-8984/1/31/015)

J. Phys.: Condens. Matter 1 (1989) 5165–5170. Printed in the UK

The effect of crystal anisotropy on the Lamb Mössbauer recoilless fraction and second-order Doppler shift in zinc

S P Tewari and Poonam Silotia
Department of Physics and Astrophysics, University of Delhi, Delhi-110007, India

Received 18 November 1988, in final form 4 January 1989

Abstract. The recently observed highly anisotropic Lamb Mössbauer recoilless fractions along the c axis and in the basal plane in a zinc crystal at temperatures of 4.2, 20.8 and 47 K are successfully explained using a dynamical model which takes into account the presence of planar modes in its dynamics. The experimental temperature-dependent second-order Doppler shifts and specific heat are also in agreement with the calculated values based on the suggested dynamical model.

1. Introduction

Mössbauer effect experiments using ^{67}Zn are highly sensitive to even a small disturbance. This is because ^{67}Zn emits a sharp ($\Gamma = 4.84\,10^{-11}$ eV) Mössbauer radiation ($E_0 =$ 93.3 keV). Zinc has a hexagonal close-packed highly anisotropic crystal structure with $c/a = 1.861$. These characteristics were successfully utilised by Potzel *et al* (1983, 1984) and Obenhuber *et al* (1987) to study amongst other factors the dynamics of zinc crystals. These workers performed the usual Mössbauer absorption experiments at different angles between the c axis and the direction of observation of γ-rays at the three temperatures 4.2, 20.8 and 47 K. (Since the Mössbauer recoilless fraction became much smaller even at 47 K, they could not perform the experiment at higher temperatures.) From the experimental data, they extracted the mean square (atomic) displacement (MSD) along the c axis and perpendicular to it. As was expected, MSD of zinc atoms and hence the Lamb Mössbauer (recoilless) fraction (LMF) were highly anisotropic. The ratio $f_\perp/f_\parallel$ increased by almost two orders of magnitude when the temperature was raised from 4.2 to 47 K. These results imply that the phonon frequency distribution function in zinc crystals should also be anisotropic. However, Potzel *et al* (1984) and Obenhuber *et al* (1987) have used two different three-dimensional isotropic Debye temperatures to characterise the dynamics of the zinc atom along the hexagonal axis and in the basal plane to explain these results.

The structure of a polymeric solid is also anisotropic but in contrast with zinc, which can be visualised as a set of weakly connected layers, a polymeric crystal consists of weakly coupled long chains of polymers. Recently an anisotropic continuum model for the collective modes of highly crystalline polymers such as polyethylene and polytetrafluoroethylene (Swaminathan *et al* 1975, Tewari and Swaminathan 1977, 1982, 1986,

0953-8984/89/315165 + 06 $02.50

Swaminathan and Tewari 1975, 1980, 1986) has been suggested and used to study various physical properties such as specific heat, anisotropic LMF, thermal neutron scattering and transport (Swaminathan *et al* 1975, Swaminathan and Tewari 1975, 1985). A two-dimensional generalisation of the model has been used to study the structural dynamics of the natural biopolymer melanins (Albanese *et al* 1984).

2. Mathematical formalism

The intensity in a Mössbauer experiment depends on the LMF f given by

$$\ln f_i = -K^2\langle U^2_{T,i}(0,0)\rangle \tag{1}$$

where $\langle U^2_{T,i}(0,0)\rangle$ is the temperature-dependent displacement–displacement autocorrelation function in the direction i, where $i = x, y, z$ and

$$K^2 = E_0^2/\hbar^2c^2.$$

The frequency distribution function $g(\nu)$ of phonons for layered structural crystals can be written as follows:

$$g(\nu) = 2g(\nu_{xy}) + g(\nu_z) \tag{2}$$

where

$$g(\nu_i) = \begin{cases} A_i\nu_i^2 & 0 \leqslant \nu \leqslant \nu_{0i} \\ B_i\nu_i & \nu_{0i} \leqslant \nu \leqslant \nu_{mi} \\ 0 & \nu > \nu_{mi} \end{cases} \tag{3}$$

where A_i and B_i are constants and can be determined using

(i) the continuity of the two distribution functions at ν_{0i},
(ii) the total number of modes along any direction is equal to N,

where N is the total number of atoms in the crystal.

$g(\nu_i)$ along the c axis, i.e. $i = z$, and $g(\nu_i)$ perpendicular to the c axis, i.e. $i = x, y$, are different because of different values of ν_{0i} and ν_{mi}.

Using equation (2), the total displacement–displacement autocorrelation function becomes

$$\langle U^2_T(0,0)\rangle = 2\langle U^2_{T,xy}(0,0)\rangle + \langle U^2_{T,z}(0,0)\rangle. \tag{4}$$

Using the dynamical model we obtain the following expression for $\langle U^2_{T,i}(0,0)\rangle$:

$$\langle U^2_{T,i}(0,0)\rangle = \frac{\hbar^2}{Mk_B\theta_{0i}}(\delta^2 - \tfrac{1}{3})^{-1}\left((\delta - \tfrac{1}{2}) + \frac{2}{\varepsilon_3^2}\int_0^{\varepsilon_3}\frac{x}{(\exp x - 1)}\,dx\right.$$
$$\left. + \frac{2}{\varepsilon_3}\int_{\varepsilon_3}^{\varepsilon_2}\frac{1}{(\exp x - 1)}\,dx\right) \tag{5}$$

where M is the mass of the vibrating unit, k_B is the Boltzmann constant, $\delta = \nu_{mi}/\nu_{0i}$, $\theta_{0i} = h\nu_{0i}/k_B$, $\theta_{mi} = h\nu_{mi}/k_B$, $\varepsilon_3 = \theta_{0i}/T$ and $\varepsilon_2 = \theta_{mi}/T$.

Using equations (5) and (1), the LMF in a given direction i can be written as

$$f_i = f_i^{3D} f_i^{2D}. \tag{6}$$

Using the suggested dynamical model, the expression for the temperature-dependent second-order Doppler (SOD) shift δ_T which is related to the velocity–velocity autocorrelation function is as follows:

$$\delta_{T,i} = \frac{3k_B T}{Mc(3\varepsilon_2^2 - \varepsilon_3^2)} \left(\frac{4\varepsilon_2^3 - \varepsilon_3^3}{24} + \frac{1}{\varepsilon_3} \int_0^{\varepsilon_3} \frac{x^3}{(\exp x - 1)} \, dx + \int_{\varepsilon_3}^{\varepsilon_2} \frac{x^2}{(\exp x - 1)} \, dx \right). \tag{7}$$

In the present model, the total specific heat C_V takes the following form:

$$C_V = 2C_{Vxy} + C_{Vz} \tag{8}$$

where C_{Vxy} and C_{Vz} denote respectively the specific heat from xy modes and z modes. The expression for any one of these modes is as follows:

$$C_{Vi} = \frac{6R}{\varepsilon_3(3\varepsilon_2^2 - \varepsilon_3^2)} \int_0^{\varepsilon_3} \frac{x^4 \exp x}{(\exp x - 1)^2} \, dx + \frac{6R}{3\varepsilon_2^2 - \varepsilon_3^2} \int_{\varepsilon_3}^{\varepsilon_2} \frac{x^3 \exp x}{(\exp x - 1)^2} \, dx. \tag{9}$$

3. Results and discussion

The anisotropic MSDs $\langle U_{T,z}^2(0,0)\rangle$ and $\langle U_{T,xy}^2(0,0)\rangle$ are calculated for different values of $(\theta_{0z}, \theta_{mz})$ and $(\theta_{0xy}, \theta_{mxy})$, respectively, at various temperatures in the range 0–47 K. For the displacement along the c axis, the characteristic temperatures $\theta_{0z} = 100$ K and $\theta_{mz} = 170$ K give the calculated values of temperature-dependent MSD in good agreement with the corresponding experimental results (Potzel *et al* 1984, Obenhuber *et al* 1987) at 4.2, 20.8 and 47 K as shown in figure 1(a). Also shown in the figure are the contributions of three- and two-dimensional modes to $\langle U_{T,z}^2(0,0)\rangle$. As is evident from the figure the contribution of two-dimensional modes is significant at all temperatures but the temperature variation is different in the two cases. In a three-dimensional Debye model such a distinction will not exist. It should be pointed out that an increase in the value of θ_{0z} or θ_{mz} results in a decrease in the value of $\langle U_{T,z}^2(0,0)\rangle$ and vice versa. However, the relative decrease or increase in $\langle U_{T,z}^2(0,0)\rangle$ is greater if θ_{mz} is increased or decreased by the same amount in comparison with the corresponding change in θ_{0z}. The calculated values of the recoilless fraction, i.e. f_z, are plotted in figure 2(a) together with the experimental results (Potzel *et al* 1984, Obenhuber *et al* 1987). The calculated values lie within the experimental error. In figure 2(a) are also shown the calculated values of $f_\parallel$ given by the modified, axially symmetric (MAS) model (Vetterling and Candela 1983) for comparison. The calculated values of $f_\parallel^{3D}$ and $f_\parallel^{2D}$ are also shown in figure 2(a). Here also, as expected, the two-dimensional contribution is significant at all temperatures.

For the displacement–displacement autocorrelation function perpendicular to the c axis, we find that the characteristic temperatures $\theta_{0xy} = 130$ K and $\theta_{mxy} = 269$ K yield values which are in good agreement with the experimental results at all the three temperatures as is shown in figure 1(b). The contributions of two-dimensional and three-dimensional modes to $\langle U_{T,xy}^2(0,0)\rangle$ are also shown. Unlike $\langle U_{T,z}^2(0,0)\rangle$, one finds that the contribution from the two-dimensional modes is larger than the contribution from the three-dimensional modes in the entire temperature range. The variation in

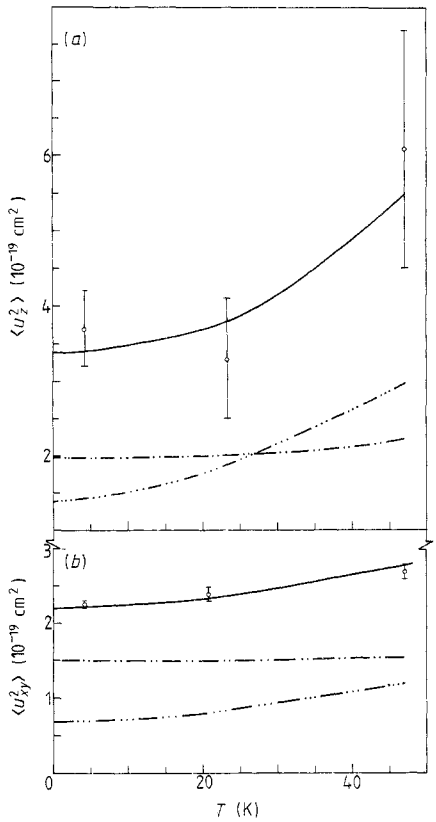

Figure 1. Comparison of the calculated values of the MSD (*a*) along the *c* axis and (*b*) in the basal plane of a zinc atom in its crystal based on the suggested dynamical model in the temperature range 0–47 K with the observed results of Potzel *et al* (1984) and Obenhuber *et al* (1987): ——, present calculations; ○, experimental results. Also shown on the figure are the contributions of the three-dimensional (—···—) and the two-dimensional (—··—) modes to $\langle U_{T,z}^2(0,0) \rangle$.

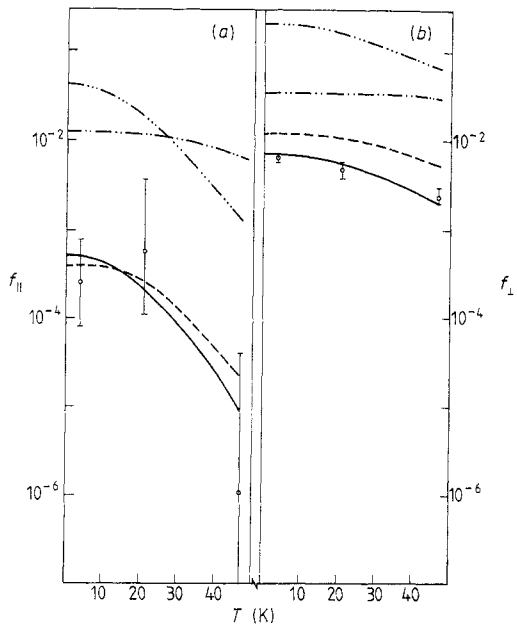

Figure 2. Comparison of LMF (*a*) along the *c* axis and (*b*) in the basal plane of a zinc atom in its crystal based on the suggested dynamical model in the temperature range 0–47 K with the observed results of Potzel *et al* (1984) and Obenhuber *et al* (1987): ——, present calculations; – – – ○, experimental results. Also shown are the results based on the MAS model (– – –) and the contributions of the three-dimensional (—···—) and the two-dimensional (—··—) modes to $f_{\parallel}$.

$\langle U_{T,xy}^2(0,0) \rangle$ with θ_{0xy} or θ_{mxy} is similar to what we have observed in $\langle U_{T,z}^2(0,0) \rangle$. However, the percentage change in the displacement in basal plane is less than the corresponding change along the hexagonal axis for a given change in the characteristic parameters. The calculated values of LMF $f_{\perp}$, i.e. f_{xy}, together with the experimental results are shown in figure 2(*b*). The agreement between the two is good. The contributions of three-dimensional and two-dimensional modes to $f_{\perp}$ are also shown in figure 2(*b*). The calculated values based on the MAS model are shown for comparison. The values of $f_{\perp}$ given by the MAS model are much larger and are not at all in agreement with the experimental results at all the three temperatures.

Using equation (7) and the values of the characteristic temperatures which explained the MSD and LMF, the SOD shifts in the temperature range 0–47 K were calculated. The computed value Δ_{SOD} of the centre shift for different temperatures compared with its value at 4.2 K are shown in figure 3, together with the experimental results (Potzel *et al*

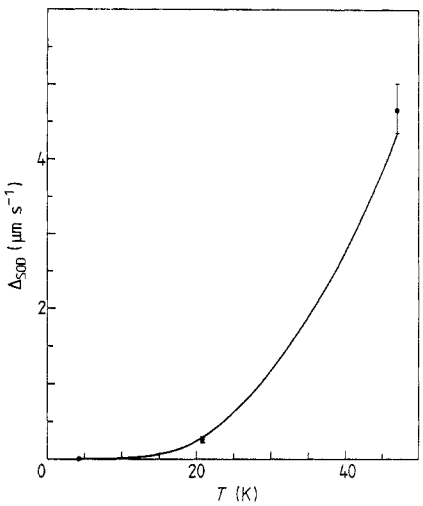

Figure 3. Comparison of the calculated temperature-dependent SOD shift based on the suggested dynamical model with the experimental values of Potzel *et al* (1984) and Obenhuber *et al* (1987) in the temperature range 0–47 K in a zinc crystal.

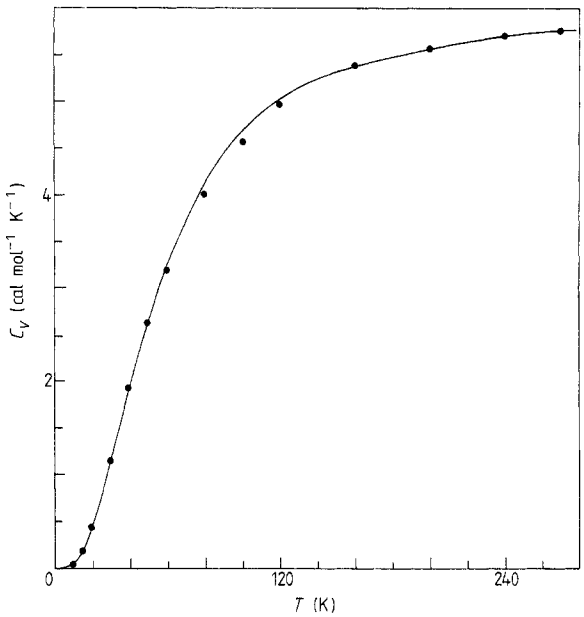

Figure 4. Comparison of the computed values of specific heat based on the proposed dynamical model with the experimental results of Martin (1968) and Eichenauer and Schulze (1959) in the temperature range 3–270 K in a zinc crystal.

1984, Obenhuber *et al* 1987). The agreement between the two is reasonably good. An analysis of our computations shows that in the SOD shift, the contribution of two-dimensional modes is much larger than the corresponding contribution of three-dimensional modes along the c axis and in the basal plane in the entire temperature range.

Using equation (9) and the values of the characteristic temperatures which explained various physical quantities such as the MSD, LMF and SOD shift, the specific heats at various temperatures have been computed and plotted in figure 4, together with the experimental results (Martin 1968, Eichenauer and Schulz 1959) in the temperature range 3–270 K. The calculated values are in reasonable agreement with the experimental results. It should be pointed out that the phonon frequency distribution function characterised by our model yields values of the specific heat closer to the experimental values (particularly at low temperatures) than those given by the extended Debye model used by Potzel *et al* and Obenhuber *et al* for $\theta_\perp = 242$ K and $\theta_\parallel = 149$ K. However, as the difference is small, it cannot be shown in the figure. Their values of specific heat calculations using $\theta_\perp = 260$ K and $\theta_\parallel = 160$ K are reproduced by our model if we change the value of θ_{0z} to 130 K without changing any other characteristic temperature of our model.

4. Conclusion

We conclude that the suggested dynamical model which incorporates the presence of planar modes is able to explain the highly anisotropic observed temperature-dependent LMF, MSD, SOD shift and specific heat in zinc crystals.

References

Albanese G, Bridelli M G and Deriu A 1984 *Biopolymers* **23** 1481–98
Eichenauer V W and Schulze M 1959 *Z. Naturf.* a **14** 28–32
Martin D L 1968 *Phys. Rev.* **167** 640–51
Obenhuber Th, Adlassnig W, Zänkert J, Närger U, Potzel W and Kalvius G M 1987 *Hyperfine Interact.* **33** 69–88
Potzel W, Adlassnig W, Narger U, Obenhuber Th, Riski K and Kalvius G M 1984 *Phys. Rev.* B **30** 4980–8
Potzel W, Narger U, Obenhuber Th, Zankert J, Adlassnig W and Kalvius G M 1983 *Phys. Lett.* **98A** 295–8
Swaminathan K and Tewari S P 1975 *Phys. Lett.* **55A** 242–4
—— 1980 *J. Polym. Sci., Polym. Phys. Edn.* **18** 1707–16
—— 1985 *Nucl. Sci. Eng.* **91** 84–94, 95–108
—— 1986 *Polym. Commun.* **27** 128–30
Swaminathan K, Tewari S P and Kothari L S 1975 *Phys. Lett.* **51A** 153–4
Tewari S P and Swaminathan K 1977 *Solid State Commun.* **24** 65–6
—— 1982 *Proc. Int. Conf. AME 1981* (New Delhi: Indian National Science Academy) pp 634–6
—— 1986 *Hyperfine Interact.* **29** 1385–8
Vetterling W T and Candela D 1983 *Phys. Rev.* B **27** 5394–403